THE ASTROPHYSICAL JOURNAL LETTERS: IN PRESS
Preprint typeset using LaTeX style emulateapj v. 11/12/01

SUPPRESSED STAR FORMATION IN CIRCUMNUCLEAR REGIONS IN SEYFERT GALAXIES

JIAN-MIN WANG, YAN-MEI CHEN, CHANG-SHUO YAN, CHEN HU AND WEI-HAO BIAN
Key Laboratory for Particle Astrophysics, Institute of High Energy Physics, CAS, 19B Yuquan Road, Beijing 100049, China
Received 2007 January 17; accepted 2007 March 30

ABSTRACT

Feedback from black hole activity is widely believed to play a key role in regulating star formation and black hole growth. A long-standing issue is the relation between the star formation and fueling the supermassive black holes in active galactic nuclei (AGNs). We compile a sample of 57 Seyfert galaxies to tackle this issue. We estimate the surface densities of gas and star formation rates in circumnuclear regions (CNRs). Comparing with the well-known Kennicutt-Schmidt (K-S) law, we find that the star formation rates in CNRs of most Seyfert galaxies are suppressed in this sample. Feedback is suggested to explain the suppressed star formation rates.

Subject headings: galaxies: active — galaxies: Seyfert — galaxies: feedback

1. INTRODUCTION

The implications of the well-known relations between black hole masses and bulge magnitudes (Magorrian et al. 1998), and the velocity dispersions (Gebhardt et al. 2000; Frarreasse & Merrit 2000) show a coevolution of the black holes and their host galaxies. However, how do black holes know the evolution stage of the galaxies and how to control the growth of the black holes are currently understood via the the feedback from the black hole (Silk & Rees 1998; Croton et al. 2006; Schawinski et al. 2006). Numerical simulations show two roles of feedback from the black hole activity: (1) modulating the star formation rates; (2) heating the medium and finally quenching the black hole activity (Di Matteo et al. 2005). The direct evidence for the presence of the feedback from active black holes has to be shown from observations, yet.

The main goal of the present paper is to show one piece of evidence for the feedback role in active galaxies. We show the AGN feedback domain, where starburst should be suppressed. We find the star formation rates in Seyfert galaxies is significantly lower than the rates predicted by the Kennicut-Schmidt's law. We use the cosmological parameters H_0 = 75km s^{-1} Mpc^{-1}, $\Omega_{\rm M}$ = 0.3 and Ω_Λ = 0.7 throughout calculations.

2. AGN FEEDBACK DOMAIN

When the CNR medium is optically thick, namely, the optical depth $\tau = \kappa_{\rm abs}\Sigma_{\rm gas} \geq 1$, where $\kappa_{\rm abs}$ is opacity and $\Sigma_{\rm gas}$ the gas surface density, the radiation from the black hole activity will continuously heat the medium and blow the gas away so as to lower the star formation rates. The condition of $\tau = 1$ yields a critical density

$$\Sigma_{\rm gas}^{c_1} = 9.0\times10^2\left(\kappa_{\rm abs}/5\right)^{-1}\ M_\odot\ {\rm pc}^{-2}, \qquad (1)$$

$\kappa_{\rm abs}$ has a mean value of 5 for the CNR medium (Semenov et al. 2003). This is feedback driven by AGN radiation. We note outflows from Seyfert active nucleus have much low kinetic luminosities, typically $\sim 10^{-(3-6)}L_{\rm Bol}$ based on X-ray warmer absorbers (Blustin et al. 2005), where $L_{\rm Bol}$ is the bolometric luminosity. Feedback from outflows could be thus neglected. When $\Sigma_{\rm gas} > \Sigma_{\rm gas}^{c_1}$, the AGN radiation-driven feedback will suppress the star formation. On the other hand, AGN feedback reaches its maximum when an AGN radiates at the Eddington limit $L_{\rm AGN} = L_{\rm Edd} = 1.3\times10^{38}(M_\bullet/M_\odot)$erg/s. In the case of $L_{\rm Edd} \leq L_{\rm SFR}^{\rm IR}$, AGN have inefficient feedback to star formation. With the help of SFR = $4.5\left(L_{\rm IR}/10^{44}{\rm erg\ s^{-1}}\right)M_\odot{\rm yr}^{-1}$, $\Sigma_{\rm gas}^{c_2}$ is given by using the K-S law $\dot\Sigma_{\rm SFR} = A\Sigma_{\rm gas}^\gamma$ (Kennicutt 1998a),

$$\Sigma_{\rm gas}^{c_2} = 8.2\times10^5 M_9^{0.7}R_{200}^{-1.4}\ M_\odot\ {\rm pc}^{-2}, \qquad (2)$$

where $\dot\Sigma_{\rm SFR} = {\rm SFR}/\pi R^2$ is the surface density of the star formation rate, $A = 2.5\times10^{-4}$, $\gamma = 1.4$, $M_9 = M_\bullet/10^9M_\odot$ is the black hole mass and $R_{200} = R/200$pc the size of the circumnuclear star forming region. When $\Sigma_{\rm gas} \geq \Sigma_{\rm gas}^{c_2}$, the gas is so dense that the luminosity from star formation dominates over the AGN. We call

$$\Sigma_{\rm gas}^{c_1} \leq \Sigma_{\rm gas} \leq \Sigma_{\rm gas}^{c_2}, \qquad (3)$$

the AGN feedback domain as shown in Fig. 1, in which the K-S law is broken.

The strong radiation pressure from the black hole accretion disk at Eddington limit is $P_{\rm AGN} \approx 1.0\times10^{-7}M_8R_{200}^{-2}$dyn cm^{-2}, where $M_8 = M_\bullet/10^8M_\odot$. The pressure from supernovae explosion is $P_{\rm SN} \approx \epsilon\dot\Sigma_{\rm SFR}c = 2.0\times10^{-8}\dot\Sigma_{\rm SFR,2}\epsilon_{-3}$dyn cm^{-2}, where $\dot\Sigma_{\rm SFR,2} = \dot\Sigma_{\rm SFR}/10^2M_\odot{\rm yr}^{-1}{\rm kpc}^{-2}$ and $\epsilon_{-3} = \epsilon/10^{-3}$ is the efficiency converting the mass into radiation (Thompson et al 2005). We find $P_{\rm AGN} \geq 5P_{\rm SN}$ within CNRs of radius $\sim$ 200pc for typical values of the parameters of ϵ, $M_\bullet$ and $\dot\Sigma_{\rm SFR}$. This indicates that the radiation from AGN dominates over the local feedback from supernovae explosion. After an AGN switches on, the star formation is suppressed and then feedback from supernovae is further weakened. The timescale of the AGN feedback to the starburst regions can be estimated by $t_{\rm FB} \sim E_{\rm gas}/f_{\rm FB}\mathcal{C}L_{\rm AGN}$, where $L_{\rm AGN}$ is AGN luminosity, $\mathcal{C} = \Delta\Omega/4\pi$ is the covering factor, the thermal energy $E_{\rm gas} \approx kTM_{\rm gas}/m_p$, k is the Boltzmann constant, m_p is the proton mass, T is the gas temperature, $M_{\rm gas} = \pi R^2\Sigma_{\rm gas}$ is the gas mass and $f_{\rm FB}$ is the feedback efficiency. We have

$$t_{\rm FB} \sim 2.6\times10^5 f_{\rm FB,-2}^{-1}R_{200}^2T_3\Sigma_{\rm gas,4}\mathcal{C}_{0.5}^{-1}L_{43}^{-1}\ \ {\rm yr}, \qquad (4)$$

where $\Sigma_{\rm gas,4} = \Sigma_{\rm gas}/10^4M_\odot$ pc^{-2}, $T_3 = T/2\times10^3$K, $f_{\rm FB,-2} = f_{\rm FB}/10^{-2}$, $L_{43} = L_{\rm AGN}/10^{43}$erg s^{-1} and $\mathcal{C}_{0.5} = \mathcal{C}/0.5$ is the covering factor of the CNRs. Such a short timescale indicates that the AGN feedback is very efficient. This is supported by a large fraction of the post-starburst AGNs in a large Sloan Digital Sky Survey sample (Kauffmann et al. 2003). The physics behind K-S law is not sufficiently understood (Thompson et al. 2005; Krumholz & McKee 2005). It is beyond the scope of the present paper to give a quantitative description of the suppressed star formation rates. Comparing Seyfert galaxies with the K-S law,

TABLE 1 THE SEYFERT GALAXY SAMPLE

Seyfert 1											
Object	Redshift	FWHM	$\log \lambda L_\lambda$	Ref.	$\log M_\bullet$	$\dot{M}_\bullet$	$\log \Sigma_{\rm gas}$	$S_{\rm PAH}$	R	$\log \dot{\Sigma}_{\rm SFR}$	
(1)	(2)	(3)	(4)	(5)	(6)	(7)	(8)	(9)	(10)	(11)	(12)
3C120	0.033	...	44.17	2	7.74[a]	0.24	4.18	76	0.48	0.85	1.32
IC4329	0.016	...	43.32	2	6.99[a]	0.03	3.70	220	0.24	1.31	1.35
MCG-2-33-34	0.014	1565	42.61	22, 5	6.11	0.01	3.13	54	0.21	0.70	1.21
MCG-5-13-17	0.013	4000	43.44	20, 1	7.50	0.04	3.92	67	0.19	0.79	1.24

NOTE.–Table 1 is published in its entirety in the electronic edition. A portion is shown here for guidance regarding its form and content.

[a] the blackhole mass are directly taken from Peterson et al. (2004).
[b] refers to [O III] FWHM.
[c] based on $M_\bullet - M_{\rm bulge}$ relation, F01475-0740: $M_{\rm bulge} = -18.80$; NGC 3660: $M_{\rm bulge} = -18.38$.

Note.-(1) source name; (2) redshift; (3) FWHM of Hβ for Seyfert 1s or stellar velocity dispersion σ for Seyfert 2s (in km s^{-1}); (4) luminosity of 5100Å deduced from extrapolation of $F_\nu \propto \nu^{-0.5}$ or [O III]λ5007Å (in erg s^{-1}); (5) references for columns (3) and (4) are given below, respectively; (6) black hole mass (in $M_\odot$); (7) accretion rate (in $M_\odot {\rm yr}^{-1}$); (8) gas surface density (in $M_\odot {\rm pc}^{-2}$); (9) surface brightness of the 3.3 μm PAH emission feature (in unit of 10^{39}ergs s^{-1}kpc^{-2}); (10) the scale of the starburst regions (in kpc); (11) and (12) are the lower ($\dot{\Sigma}^{\rm L}_{\rm SFR}$) and upper ($\dot{\Sigma}^{\rm U}_{\rm SFR}$) limits of surface density of star formation rates, respectively (in $M_\odot {\rm yr}^{-1}{\rm kpc}^{-2}$).

Reference.-(1) NED; (2) Peterson et al. (2004); (3) Spinogilio et al. (1995); (4) Doroshenko & Terebezh (1979); (5) Kinney et al. (1993); (6) Nelson & Whittle (1995); (7) Dahari & Robertis (1988); (8) Lipari et al. (1991); (9) Corral et al. (2005); (10) Kirhakos & Steiner (1990); (11) Visvanathan & Griersmith (1977); (12) Cid Fernandes et al. (2004); (13) Gu & Huang (2002); (14) Kailey & Lebofsky (1988); (15) Heraudeau & Simien (1998); (16) Bassani (1999); (17) Whittle et al. (1988); (18) Whittle (1992); (19) Garcia-Rissmann et al. (2005); (20) Crenshaw et al. (2003); (21) Marzini et al. (2003); (22) Veron-Cetty et al. (2001); (23) Postman & Lauer (1995).

a universal rule of cosmic star formation, we may get the undergoing physics in the CNRs.

We have to point out here that the short feedback time does NOT mean the same timescale of the starburst. The present $t_{\rm FB}$ means the starburst rates will be suppressed once AGN is triggered and make it possible for AGN and starburst coexist.

3. APPEARANCE OF FEEDBACK IN SEYFERT GALAXIES

For the goal to test the above scenario, we compile 57 Seyfert galaxies (Imanishi 2002; Imanishi 2003; Imanishi & Wada 2004). The star formation rates in CNRs of Seyfert galaxies can be traced by several indicators, particularly, PAH features at 3.3, 6.2, 7.7, 8.6 and 11.2μm, which radiate from vibration of PAH grains containing about 50 carbon atoms. Among the features, 3.3μm emission is intrinsically strong and less affected by broad silicate dust absorption (Imanishi 2002). We choose 3.3μm emission as an indicator of the star formation rate. We convert the PAH emission into IR luminosity via $L_{\rm IR} = 10^3 L_{\rm PAH}$ relation with a scatter by a factor of 2-3 for pure star formation (Imanishi 2002). Since some PAH grains would be destroyed by EUV and X-ray photons from the central engine, we have the lower limit of the surface density of the star formation rates

$$\dot{\Sigma}^{\rm L}_{\rm SFR} = 35.8 L_{\rm PAH,41} R^{-2}_{200}\ (M_\odot {\rm yr}^{-1}{\rm kpc}^{-2}), \quad (5)$$

by using the relation of the star formation rate and the infrared luminosity (eq. 7) (Kennicutt 1998a), where $L_{\rm PAH,41} = L_{\rm PAH}/10^{41}{\rm erg\ s}^{-1}$. On the other hand, the infrared emission from Seyfert galaxies covers the contribution from starburst and reprocessing radiation from AGNs, we have the upper limit of the surface density of the star formation rates

$$\dot{\Sigma}^{\rm U}_{\rm SFR} = 35.8 L_{\rm FIR,44} R^{-2}_{200}\ (M_\odot {\rm yr}^{-1}{\rm kpc}^{-2}), \quad (6)$$

where $L_{\rm FIR,44} = L_{\rm FIR}/10^{44}{\rm erg\ s}^{-1}$ is the observed far-IR luminosity. We take the geometric average $\dot{\Sigma}_{\rm SFR} = \left(\dot{\Sigma}^{\rm L}_{\rm SFR}\dot{\Sigma}^{\rm U}_{\rm SFR}\right)^{1/2}$ and the error bars correspond to $\dot{\Sigma}^{\rm L}_{\rm SFR}$ and $\dot{\Sigma}^{\rm U}_{\rm SFR}$. We have to stress this average only represents the central value of logarithm of $\dot{\Sigma}^{\rm U}_{\rm SFR}$ and $\dot{\Sigma}^{\rm L}_{\rm SFR}$ and the upper and lower limits of $\dot{\Sigma}_{\rm SFR}$ are the most important. Table 1 gives the sample of Seyfert galaxies, which have been observed through IRTF SpeX or Subaru IRCS with spatial resolution of $0.9'' - 1.6''$.

For Seyfert 1 galaxies, we estimate $L_{\rm Bol} = 9L_{5100}$, where L_{5100} is the luminosity at 5100Å and then the accretion rate $\dot{M}_\bullet = L_{\rm Bol}/\eta c^2$, where $\eta = 0.1$ is the accretion efficiency. The black hole masses are estimated from the empirical relation of reverberation mapping (Kaspi et al. 2000), or directly taken from the mapping (Peterson et al. 2004). We assume that the potential of the total mass within the CNRs controls the massive disk fueling to the black hole, where star formations are taking place either. Assuming the Keplerian rotation, the surface density of the disk is

$$\Sigma_{\rm tot} = 2.1\times10^6 \alpha_{0.1}^{-4/5} \dot{M}_{\bullet,1}^{3/5} f_\bullet^{-1/5} M_8^{1/5} R_{200}^{-3/5}\quad M_\odot\ {\rm pc}^{-2}, \quad (7)$$

given by the disk model (King et al. 2002; Yi & Blackman 1994; Tan 2005), where the opacity $\kappa_{\rm abs} = 5$ in this region, $f_\bullet$ is the ratio of the black hole mass to the total, $\dot{M}_{\bullet,1} = \dot{M}_\bullet/1.0 M_\odot {\rm yr}^{-1}$ and $\alpha_{0.1} = \alpha/0.1$ is the viscosity (Shakura & Sunyaev 1973). This estimation is the lower limit since we replace the infalling mass rates in CNRs by black hole accretion rates. The gas surface density of the disk $\Sigma_{\rm gas} = f_{\rm g}\Sigma_{\rm tot}$

$$\Sigma_{\rm gas} = 1.0\times10^5 f_{\rm g,0.05} \alpha_{0.1}^{-4/5} \dot{M}_{\bullet,1}^{3/5} f_\bullet^{-1/5} M_8^{1/5} R_{200}^{-3/5}\quad M_\odot\ {\rm pc}^{-2}, \quad (8)$$

where $f_{\rm g,0.05} = f_{\rm g}/0.05$ is the gas fraction to the total. Considering the disk is located inside the bulge, we have $f_{\rm g} = M_{\rm gas}/M_{\rm disk} > M_{\rm gas}/M_{\rm Bulge} = \left(M_{\rm gas}/M_{\rm dust}\right)\left(M_{\rm dust}/M_\bullet\right)\left(M_\bullet/M_{\rm Bulge}\right)$, where $M_{\rm disk}$ is the total mass of the disk, $M_{\rm gas}/M_{\rm dust}$ is the gas-to-dust mass ratio and $M_{\rm Bulge} \approx 10^3 M_\bullet$ is the bulge mass (Kormendy & Gebhardt 2001; McLure & Dunlop 2002). It has been found that the dust mass in PG quasars is comparable with in Seyfert galaxies (Spinoglio et al. 2002; Haas et

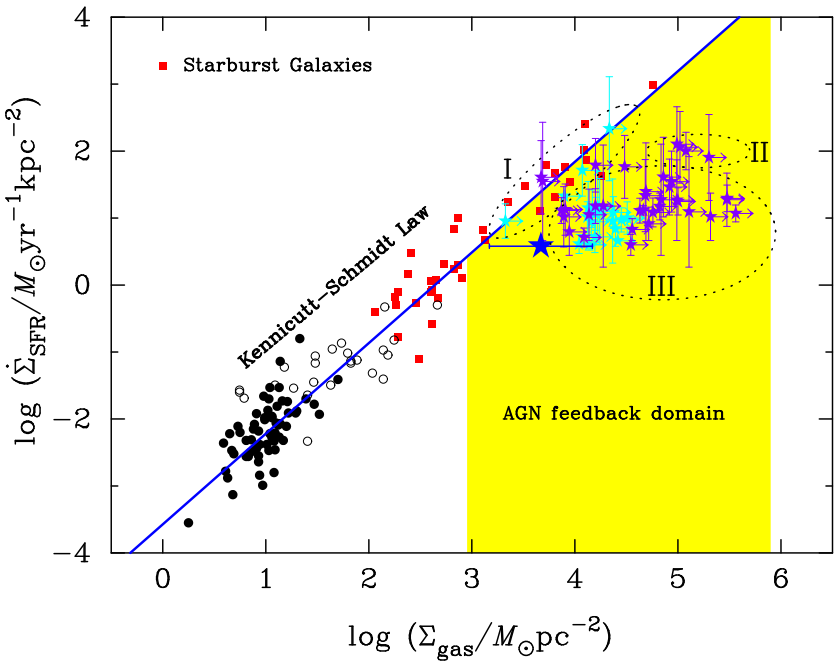

FIG. 1.— The plot of gas and star formation rate surface densities. The yellow region is the AGN feedback domain given by $\Sigma_{\rm gas}^{c_1} \leq \Sigma_{\rm gas} \leq \Sigma_{\rm gas}^{c_2}$. The Compton thick region has $\Sigma_{\rm gas} \geq 8.0\times10^3 M_\odot$ pc^{-2} (i.e. $N_{\rm H} \geq 10^{24}$cm^{-2}). The red squares are starburst galaxies taken from Kennicutt (1998b). The cyan and blue-magenta stars are Seyfert 1 and 2 galaxies, respectively. The blue star is NGC 3227, in which the star formation rate is $0.05 M_\odot$ yr^{-1} and the gas mass $M_{\rm gas} = (2-20)\times10^8 M_\odot$ within 65pc taken from Davies et al. (2006).

al. 2003). The mean value of gas-to-dust mass ratio is $\langle M_{\rm gas}/M_{\rm dust}\rangle \sim 250$ (Haas et al. 2003). We estimated dust mass from $M_{\rm dust} \sim 4.78 f_{100\mu} D_{\rm L}^2 \left[\exp(143.38/T_{\rm dust})-1\right] M_\odot$, and the dust temperature is estimated by $T_{\rm dust} = (1+z)\left[0.5-82/\ln(0.3 f_{60\mu}/f_{100\mu})\right]$K, where $f_{100\mu}$ and $f_{60\mu}$ are the fluxes at $100\mu m$ and $60\mu m$ in unit of Jy, respectively, $D_{\rm L}$ is the luminosity distance in unit of Mpc (Evans et al. 2005). We find the mean value of $\langle M_{\rm dust}/M_\bullet\rangle = 0.2\pm0.2$ in our sample. So we have $f_{\rm g} \geq 0.05$ as a lower limit in this paper. Thompson et al. (2005) used $f_{\rm g} = 0.1$. We note $\Sigma_{\rm gas} \propto f_\bullet^{-1/5}$, resulting in uncertainties of $\Sigma_{\rm gas}$ by a factor of 4 for $f_\bullet = 10^{-3}-1$. $\alpha = 0.1$ is used for all Seyfert galaxies.

For Seyfert 2 galaxies, dusty tori obscure the active regions. We estimate the bolometric luminosity from $L_{\rm Bol} = 3500 L_{[\rm O\ III]}$ with a mean uncertainty of 0.38 dex (Heckman et al. 2004), where $L_{[\rm O\ III]}$ is the [O III]λ5007 luminosity, and hence the black hole accretion rates. The black hole masses are estimated through the $M_\bullet - \sigma$ relation (Tremaine et al. 2002), where the dispersion velocity $\sigma = {\rm FWHM([O\ III])}/2.35$ if the dispersion velocity is not available.

Fig. 1 shows the $\Sigma_{\rm gas} - \dot{\Sigma}_{\rm SFR}$ plot of Seyfert CNRs. We find that CNR gas surface densities of Seyfert galaxies are located within the AGN feedback domain. There are clearly three branches in the figure, separating the Seyfert galaxies, when $\Sigma_{\rm gas}^{c_2} > \Sigma_{\rm gas} > \Sigma_{\rm gas}^{c_1}$. Seyfert galaxies marked in Zone I still satisfy the K-S law. Those (Mrk 273, Mrk 938, NGC 5135 and NGC 1068) marked in Zone II are located between the K-S law and Zone III. These are ultra-luminous infrared galaxies, or mixed with strong starbursts. The main energy sources in the CNRs are in a transition state from a starburst to an AGN in these galaxies. The fraction of the transiting galaxies is only $4/57 \sim 1/10$. Though the completeness of the present sample is uncertain, this fraction implies that the transition is quite short and indicated by the feedback timescale from equation (4). The Seyfert galaxies in Zone III are undergoing suppressed star formation strongly, being 1-2 orders lower than that predicted by the K-S law. The suppressed $\dot{\Sigma}_{\rm SFR}$ is obviously caused by the feedback. Galaxies obeying the K-S law are powered by nuclear energy from stars, however gravitational energy released from accretion onto the black holes is powering AGNs if a transition from starburts to active galaxies happens. With the dissipation of CNR gas due to star formation and accretion onto the black holes, $\Sigma_{\rm gas}$ is decreasing and the galaxies may return to the K-S law once AGNs switch off. Such a behavior likes evolution of stellar energy sources in the Hertzprung-Russell diagram.

It has been found that black hole duty cycles follow the history of star formation rate density (Wang et al. 2006). The above scenario then implies that both the black hole activities and starbursts are episodic (Davies et al. 2006). The multiple cycles of the black holes and starbursts make it impossible to measure the time delay between the two episodes. However the stellar synthesis may tell the star formation history and then give the black hole activity history.

4. CONCLUSIONS AND DISCUSSIONS

We find direct evidence for the feedback from active black holes in Seyfert galaxies. Once a black hole is triggered, the feedback will significantly suppress the starbursts within a quite short timescale of a few 10^5years. The duty cycles of Seyfert galaxies strongly indicate there is an efficient way to frequently trigger black holes and quench starbursts.

The data presented in this paper are only lower limits of the gas densities. Future VLT (Very Large Telescope) and ALMA (Atacama Large Millimiter Array) measurements of the star formation rates and gas densities will finally identify roles of the feedback from the black hole activities.

The helpful comments from the referee are acknowledged. The authors are grateful to R. C. Kennicutt, L. C. Ho, S. N. Zhang and X.-Y. Xia for useful discussions. We appreciate the stimulating discussions among the members of IHEP (Institute of High Energy Physics) AGN group. J.-M.W. thanks the Natural Science Foundation of China for support via NSFC-10325313 and 10521001, CAS key project via KJCX2-YW-T03.

REFERENCES

Bassani, L., et al. 1999 ApJS, 121, 473
Blustin, A. J., Page, M. J., Fuerst, S. V., Branduardi-Raymont, G., Ashton, C. E. 2005, A&A, 431, 111
Cid Fernandes, R., et al. Rodrigues Lacerda, R.; Joguet, B. 2004 MNRAS, 355, 273
Crenshaw, D. M., Kraemer, S. B. & Gabel, J. R. 2003 ApJ, 126, 1690
Croton, D. J., Springel, V., White, S. D. M., De Lucia, G., Frenk, C. S., Gao, L., Jenkins, A., Kauffmann, G., Navarro, J. F., Yoshida, N. 2006, MNRAS, 365, 11
Corral, A., Barcons, X., Carrera, F. J., Ceballos, M. T., Mateos, S. 2005 A&A, 431, 97
Dahari, O. & Robertis, M. M. D. 1988 ApJS, 67, 249
Davies, R. I., et al. 2006, ApJ, 646, 754
Doroshenko, V. T. & Terebezh, V. Yu. 1979 SvAL, 5, 305
Di Matteo, T., Springel, V., Hernquist, L. 2005, Nature, 433, 604
Evans, A. S., Mazzarella, J. M., Surace, J. A., Frayer, D. T., Iwasawa, K. & Sanders, D. B. 2005, ApJS, 159, 197
Ferrarese, L. & Merritt, D., 2000, ApJ, 539, L9
Garcia-Rissmann, A., Vega, L. R.; Asari, N. V.; Cid Fernandes, R.; Schmitt, H.; Gonzoulez Delgado, R. M.; Storchi-Bergmann, T. 2005 MNRAS, 359, 765
Gebhardt, K. et al., 2000, ApJ, 543, L5
Gu, Q. & Huang, J. 2002 ApJ, 579, 205
Haas, M., et al. 2003, A&A, 402, 87
Heckman, T. M. et al. 2004, ApJ, 613, 109
Heraudeau, P. & Simien, F. 1998 A&AS, 133, 317
Imanishi, M., 2002, ApJ, 569, 44
Imanishi, M. 2003, ApJ, 599, 918
Imanishi, M. & Wada, K. 2004, ApJ, 617, 214
Kailey, W. F. & Lebofsky, M. J. 1988 ApJ, 326, 653
Kaspi, S., Smith, P. S., Netzer, H., Maoz, D., Jannuzi, B. T., Giveon, U., 2000, ApJ, 533, 631
Kauffmann, G., et al. 2003, MNRAS, 346, 1055
Kennicutt, R. C., Jr. 1998a, ARA&A, 36, 189
Kennicutt, R. C. Jr. 1998b, ApJ, 498, 541
King, A., Frank, J. & Raine, D. J., 2002, Accretion Power in Astrophysics, Cambridge University Press, p.90
Kinney, A. L., Bohlin, R. C., Calzetti, D., Panagia, N., & Wyse, R. F. G. 1993 ApJS, 86, 5
Kirhakos, S. D. & Steiner, J. E. 1990 AJ, 99, 1722
Kormendy, J. & Gebhardt, K., 2001, in The 20th Texas Symposium on Relativistic Astrophysics, ed. H. Martel & J.C. Wheeler, AIP, (astro-ph/0105230)
Krumholz, M. R. & McKee, C. F. 2005, ApJ, 630, 250
Lipari, S., Bonatto, C. & Pastoriza, M. 1991 MNRAS, 253, 19
Magorrian, J. et al., 1998, AJ, 115, 2285
Marzini, P., Sulentic, J. W., Zamanov, R., Calvani, M. & Dultzin-Hacyan, D., 2003 ApJS, 145, 199
McLure, R. J. & Dunlop, J. S. 2002, MNRAS, 331, 795
Nelson, C. H. & Whittle, M. 1995 ApJS, 99, 67
Peterson, B. M. et al. 2004, ApJ, 613, 682
Postman, M., Lauer, T. R. 1995 ApJ, 440, 28
Silk, J. & Rees, M. J. 1998, A&A, 331, L1
Schawinski, K., et al. 2006, Nature, 442, 888
Semenov, D., Henning, Th., Helling, Ch., Ilgner, M., Sedlmayr, E. 2003, A&A, 410, 611
Shakura, N. I. & Sunyaev, R. A. 1973, A&A, 24, 337
Spinoglio, L., Andreani, P., Malkan, M. A. 2002, ApJ, 572, 105
Spinoglio, L., Malkan, M. A., Rush, B., Carrasco, L. & Recillas-cruz, E. 1995 ApJ, 453, 616
Tan, J. C. & Blackman, E. G. 2005, MNRAS, 362, 983
Thompson, T. A., Quataert, E., Murray, N. 2005, ApJ, 630, 167
Tremaine, S. et al. 2002, ApJ, 574, 740
Veron-Cetty, M.-P., Veron, P. & Gongalves, A.C. 2001 A&A, 372, 730
Visvanathan, N., Griersmith, D. 1977 A&A, 59, 317
Wang, J.-M., Chen, Y.-M. & Zhang, F. 2006, ApJ, 647, L17
Whittle, M. 1992 ApJS, 79, 49
Whittle, M., Pedlar, A., Meurs, E. J. A., Unger, S. W., Axon, D. J. & Ward, M. J. 1988 ApJ, 326, 125
Yi, I., Field, G. B. & Blackman, E. G. 1994, ApJ, 432, L31

Table 1 The Seyfert Galaxy Sample

Seyfert 1											
Object	Redshift	FWHM	$\log \lambda L_\lambda$	Ref.	$\log M_\bullet$	$\dot{M}_\bullet$	$\log \Sigma_{\rm gas}$	$S_{\rm PAH}$	R	$\log \dot{\Sigma}_{\rm SFR}$	
(1)	(2)	(3)	(4)	(5)	(6)	(7)	(8)	(9)	(10)	(11)	(12)
3C120	0.033	...	44.17	2	7.74[a]	0.24	4.18	76	0.48	0.85	1.32
IC4329	0.016	...	43.32	2	6.99[a]	0.03	3.70	220	0.24	1.31	1.35
MCG-2-33-34	0.014	1565	42.61	22, 5	6.11	0.01	3.13	54	0.21	0.70	1.21
MCG-5-13-17	0.013	4000	43.44	20, 1	7.50	0.04	3.92	67	0.19	0.79	1.24
Mrk79	0.022	...	43.72	2	7.72[a]	0.08	4.00	71	0.32	0.82	1.31
Mrk335	0.025	...	43.86	2	7.15[a]	0.14	3.94	36	0.37	0.52	0.68
Mrk509	0.035	...	44.28	2	8.15[a]	0.30	4.31	62	0.51	0.76	1.24
Mrk530	0.029	6560	44.04	20, 1	8.35	0.17	4.25	67	0.42	0.79	1.15
Mrk618	0.035	3018	44.00	21, 4	7.65	0.16	4.04	44	0.51	0.61	1.59
Mrk704	0.030	5684	43.53	21, 1	7.88	0.05	3.84	32	0.44	0.47	0.76
Mrk817	0.031	...	43.82	2	7.69[a]	0.11	3.97	78	0.45	0.86	1.42
Mrk1239	0.019	1075	43.84	22, 3	6.65	0.11	4.02	47	0.17	0.64	1.70
NGC863	0.027	...	43.81	2	7.68[a]	0.10	4.00	33	0.40	0.48	0.95
NGC931	0.016	1830	43.70	20, 1	7.01	0.08	3.93	61	0.24	0.75	1.55
NGC2639	0.011	3100	43.77	20, 1	7.51	0.09	4.17	23	0.16	0.33	1.58
NGC4235	0.008	7600	43.51	20,11	8.11	0.05	4.22	49	0.12	0.66	0.66
NGC4253	0.013	1630	43.41	20, 4	6.70	0.04	3.87	230	0.12	1.33	2.10
NGC5548	0.017	...	43.51	2	7.83[a]	0.05	3.96	61	0.26	0.75	1.14
NGC5940	0.034	5240	44.07	20, 1	8.18	0.19	4.20	41	0.49	0.58	1.10
NGC7469	0.016	...	43.72	2	7.08[a]	0.08	4.14	390	0.12	1.56	3.11
Seyfert 2											
Object	Redshift	σ	$\log L_{\rm [O\ III]}$	Ref.	$\log M_\bullet$	$\dot{M}_\bullet$	$\log \Sigma_{\rm gas}$	$S_{\rm PAH}$	R	$\log \dot{\Sigma}_{\rm SFR}$	
(1)	(2)	(3)	(4)	(5)	(6)	(7)	(8)	(9)	(10)	(11)	(12)
F01475-0740	0.017	...	41.69	13	7.55[c]	0.30	4.36	50	0.26	0.66	0.99
F04385-0828	0.015	907[b]	40.12	7,13	8.77	0.01	3.71	60	0.22	0.74	1.51
F15480-0344	0.030	664[b]	42.95	8,13	8.22	5.46	5.12	50	0.43	0.66	1.37
IC3639	0.011	95	42.11	19,13	6.83	0.80	4.66	113	0.13	1.02	2.21
MCG-3-34-64	0.017	155	42.32	12,13	7.69	1.30	4.79	50	0.24	0.66	1.87
Mrk34	0.015	570[b]	43.04	7, 7	7.96	6.78	5.36	95	0.17	0.94	1.20
Mrk78	0.037	172	42.22	6,17	7.87	1.03	4.63	102	0.41	0.97	1.37
Mrk273	0.038	211	42.39	19,16	8.22	1.52	4.79	377	0.42	1.54	2.66
Mrk334	0.022	250[b]	41.29	7,13	6.52	0.12	4.00	265	0.19	1.39	2.19
Mrk463	0.051	545[b]	43.44	18,18	7.88	16.82	5.28	81	0.56	0.88	1.67
Mrk477	0.038	370[b]	43.54	18,13	7.20	21.57	5.28	135	0.42	1.10	1.49
Mrk573	0.017	123	42.00	6,13	7.28	0.62	4.52	50	0.24	0.66	1.16
Mrk938	0.019	330[b]	42.77	7,13	7.00	3.66	4.88	570	0.28	1.72	2.28
Mrk993	0.015	392[b]	40.87	9,7	7.30	0.05	3.86	30	0.22	0.44	0.82
NGC262	0.015	118	41.91	6,13	7.21	0.51	4.47	120	0.22	1.04	1.19
NGC513	0.020	152	40.60	6,13	7.65	0.02	3.69	40	0.30	0.57	1.47
NGC1068	0.004	151	42.65	6,13	7.64	2.73	5.10	198	0.15	1.26	2.55
NGC1194	0.013	396[b]	40.84	10,14	7.32	0.04	3.89	40	0.19	0.57	0.85
NGC1241	0.014	136	42.47	19,13	7.46	1.83	4.91	20	0.18	0.27	1.92
NGC1320	0.010	116	40.96	6,13	7.18	0.06	4.00	90	0.15	0.92	1.44
NGC1667	0.015	173	41.91	6,13	7.88	0.51	4.64	30	0.19	0.44	2.10
NGC2992	0.008	158	41.92	6,16	7.72	0.52	4.74	133	0.12	1.09	2.00
NGC3660	0.012	...	40.91	13	7.33[c]	0.05	3.94	50	0.19	0.66	1.43
NGC3786	0.009	142	41.52	6, 7	7.53	0.20	4.43	91	0.13	0.92	1.30
NGC4388	0.008	119	41.68	6,13	7.22	0.30	4.49	50	0.12	0.66	2.12
NGC4501	0.008	171	39.80	15,13	7.86	0.01	3.49	50	0.12	0.66	2.43
NGC4968	0.010	105	42.37	19,16	7.01	1.44	4.79	120	0.15	1.04	1.45
NGC5135	0.014	128	42.31	19,13	7.35	1.26	4.82	360	0.16	1.52	2.59
NGC5252	0.023	190	41.96	6,13	8.04	0.57	4.56	80	0.33	0.87	1.30
NGC5256	0.028	315[b]	41.85	7,13	6.92	0.44	4.29	214	0.31	1.30	2.23
NGC5347	0.008	93	40.45	6,13	6.79	0.02	3.67	90	0.12	0.92	1.31
NGC5674	0.025	129	41.87	19,16	7.36	0.45	4.49	68	0.21	0.80	1.87
NGC5695	0.014	144	40.50	6,13	7.56	0.02	3.75	30	0.18	0.44	1.14
NGC5929	0.008	121	40.96	6,13	7.25	0.06	4.08	20	0.12	0.27	2.09
NGC7172	0.009	154	39.77	19,13	7.67	0.01	3.47	125	0.10	1.06	2.16
NGC7674	0.029	144	42.49	6,13	7.56	1.93	4.72	120	0.42	1.04	1.88
NGC7682	0.017	123	41.72	6,13	7.28	0.32	4.35	30	0.24	0.44	0.76

[a]the blackhole mass are directly taken from Peterson et al. (2004).
[b]refers to [O III] FWHM.
[c]based on $M_\bullet - M_{\rm bulge}$ relation, F01475-0740: $M_{\rm bulge}$ = –18.80; NGC 3660: $M_{\rm bulge}$ = –18.38.

Note.-(1) source name; (2) redshift; (3) FWHM of Hβ for Seyfert 1s or stellar velocity dispersion σ for Seyfert 2s (in km s^{-1}); (4) luminosity of 5100Å deduced from extrapolation of $F_\nu \propto \nu^{-0.5}$ or [O III]λ5007Å (in erg s^{-1}); (5) references for columns (3) and (4) are given below, respectively; (6) black hole mass (in $M_\odot$); (7) accretion rate (in $M_\odot$yr^{-1}); (8) gas surface density (in $M_\odot$pc^{-2}); (9) surface brightness of the 3.3 μm PAH emission feature (in $\times 10^{39}$ergs s^{-1}kpc^{-2}); (10) the scale of the starburst regions (in kpc); (11) and (12) are the lower ($\dot{\Sigma}^{\rm L}_{\rm SFR}$) and upper ($\dot{\Sigma}^{\rm U}_{\rm SFR}$) limits of surface density of star formation rates, respectively (in $M_\odot$yr^{-1}kpc^{-2}).

Reference.-(1) NED; (2) Peterson et al. (2004); (3) Spinogilio et al. (1995); (4) Doroshenko & Terebezh (1979); (5) Kinney et al. (1993); (6) Nelson & Whittle (1995); (7) Dahari & Robertis (1988); (8) Lipari et al. (1991); (9) Corral et al. (2005); (10) Kirhakos & Steiner (1990); (11) Visvanathan & Griersmith (1977); (12) Cid Fernandes et al. (2004); (13) Gu & Huang (2002); (14) Kailey & Lebofsky (1988); (15) Heraudeau & Simien (1998); (16) Bassani (1999); (17) Whittle et al. (1988); (18) Whittle (1992); (19) Garcia-Rissmann et al. (2005); (20) Crenshaw et al. (2003); (21) Marzini et al. (2003); (22) Veron-Cetty et al. (2001); (23) Postman & Lauer (1995).

1. NASA/IPAC Extragalatic Database
2. Peterson, B. M., et al. 2004 ApJ, 613, 682
3. Spinoglio, L., Malkan, M. A., Rush, B., Carrasco, L. & Recillas-cruz, E. 1995 ApJ, 453, 616
4. Doroshenko, V. T. & Terebezh, V. Yu. 1979 SvAL, 5, 305
5. Kinney, A. L., Bohlin, R. C., Calzetti, D., Panagia, N., & Wyse, R. F. G. 1993 ApJS, 86, 5
6. Nelson, C. H. & Whittle, M. 1995 ApJS, 99, 67
7. Dahari, O. & Robertis, M. M. D. 1988 ApJS, 67, 249
8. Lipari, S., Bonatto, C. & Pastoriza, M. 1991 MNRAS, 253, 19
9. Corral, A., Barcons, X., Carrera, F. J., Ceballos, M. T., Mateos, S. 2005 A&A, 431, 97
10. Kirhakos, S. D. & Steiner, J. E. 1990 AJ, 99, 1722
11. Visvanathan, N., Griersmith, D.1977 A&A, 59,317
12. Cid Fernandes, R., et al. 2004 MNRAS, 355, 273
13. Gu, Q. & Huang, J. 2002 ApJ, 579, 205
14. Kailey, W. F. & Lebofsky, M. J. 1988 ApJ, 326, 653
15. Heraudeau, P. & Simien, F. 1998 A&AS, 133, 317
16. Bassani, L., et al. 1999 ApJS, 121, 473
17. Whittle, M., et al. 1988 ApJ, 326, 125
18. Whittle, M. 1992 ApJS, 79, 49
19. Garcia-Rissmann, A., et al. 2005 MNRAS, 359, 765
20. Crenshaw, D. M., Kraemer, S. B. & Gabel, J. R. 2003 ApJ, 126, 1690
21. Marzini, P., et al. 2003 ApJS, 145, 199
22. Veron-Cetty, M.-P., Veron, P. & Gongalves, A.C. 2001 A&A, 372, 730
23. Postman, M., & Lauer, T. R. 1995 ApJ, 440, 28